

# Modeling of the Hydro-Sedimentary Dynamics of the Coastal and Port Area of Pointe-Noire (Republic of Congo)

Westinevy Benarez Ndzessou<sup>1,2\*</sup>, Destin Gemetone Etou<sup>2</sup>, Toudissa Gertrud Rita Mayoukou<sup>1,2</sup>, Elombo Motoula Smaël Magloire<sup>1,2</sup>, Merge Mbali<sup>1,2</sup>, Christian Armand Anicet Tathy<sup>2</sup>

<sup>1</sup>Higher Institute of Architecture, Urban Planning, Building, and Public Works, Denis SASSOU NGUESSO University, Brazzaville, Republic of the Congo

<sup>2</sup>Mechanics, Energy, and Engineering Laboratory of the National Polytechnic School, Marien NGOUABI University, Brazzaville, Republic of the Congo

Email: \*benarezndzessou@gmail.com

**How to cite this paper:** Ndzessou, W.B., Etou, D.G., Mayoukou, T.G.R., Magloire, E.M.S., Mbali, M. and Tathy, C.A.A. (2026) Modeling of the Hydro-Sedimentary Dynamics of the Coastal and Port Area of Pointe-Noire (Republic of Congo). *Open Journal of Marine Science*, 16, 1-26. <https://doi.org/10.4236/ojms.2026.161001>

**Received:** October 2, 2025

**Accepted:** November 28, 2025

**Published:** December 1, 2025

Copyright © 2026 by author(s) and Scientific Research Publishing Inc.

This work is licensed under the Creative Commons Attribution International License (CC BY 4.0).

<http://creativecommons.org/licenses/by/4.0/>



Open Access

## Abstract

The coastal zone of Pointe-Noire, located on the Atlantic coast of the Republic of Congo, is subject to complex hydro-sedimentary dynamics influenced by ocean currents, waves and tides. This article presents the numerical modeling of the hydro-sedimentary dynamics of the Pointe-Noire coastal zone using two tools from the integrated CMS (Coastal Modeling System) modeling system: CMS-Wave, which is a wave model, and CMS-Flow, a coupled current and sediment transport model. Analysis of the test case results revealed the highest wave and current amplitudes near the Songolo coast (northern zone) and also along the outer breakwater protecting the port (southern zone). These currents are responsible for erosion in Loango Bay. Sediment movement is activated solely by wave breaking and drained by the drift currents they generate. On the southern side of the port, sediment is transported along the outer breakwater towards the north, fed by sand from the Sauvage coast. This sand transit is responsible for the excessive filling of the sand trap area. On the north side of the port, transport flows downhill toward the port enclosure, fed by the Songolo vouchers. The volume of sediment moved within a model area of 345.6 km<sup>2</sup> over a period of one month is approximately 15775.5 m<sup>3</sup>. The study provided a better understanding of the mechanisms at play in order to support sustainable coastal management and port development strategies.

## Keywords

Hydrodynamics, Hydro-Sedimentary, Swell, CMS-Flow, CMS-Wave, Tide, Marine Current

## 1. Introduction

The coastal area of Pointe-Noire is crucial to the economic development of the Republic of Congo due to the presence of the country's main deep-water port and is also a source of livelihood for the coastal population. This coastal area has specific hydro-sedimentary characteristics that are significantly influenced by wave propagation and tidal fluctuations. This process is the source of strong natural and anthropogenic pressure, which is reflected in particular by coastal erosion in Louango Bay and intense sediment transport, leading to excessive silting of the access channel to the port of Pointe-Noire [1]-[3]. The objective of this study is to model hydro-sedimentary dynamics in order to identify the specific characteristics of this site and anticipate phenomena that could disrupt the proper functioning of port facilities and the coastal environment. The analysis method is based on the integrated numerical modeling system known as the Coastal Modeling System (CMS) [4]-[8]. This approach made it possible to assess the involvement of each of the oceanic forcings in the dynamics of the coastal process in this coastal zone.

## 2. Data and Method

### 2.1. Study Area

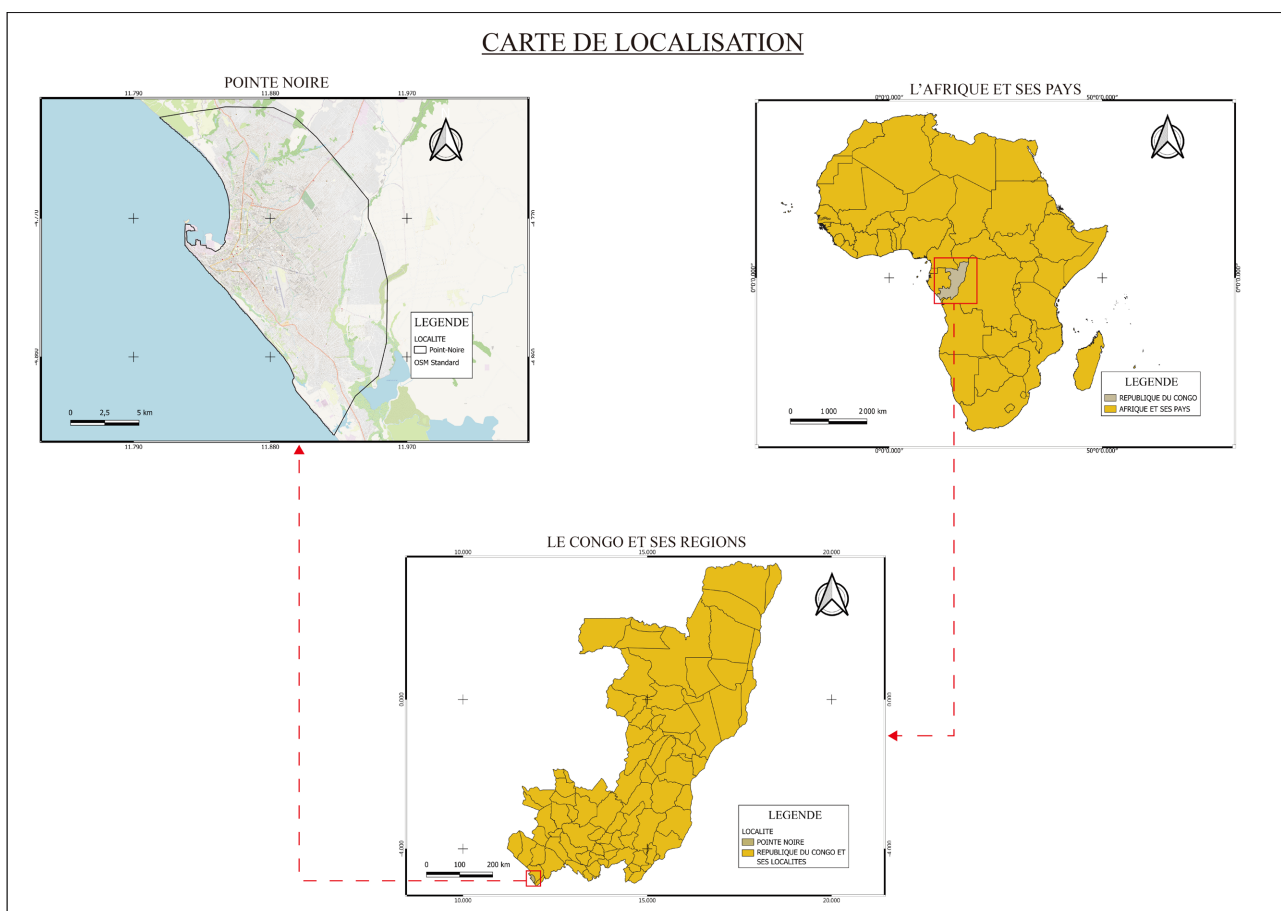


Figure 1. Coastal area of Pointe-Noire.

The coastal area covered by this study is a 170 km stretch of coastline that includes the Autonomous Port of Pointe-Noire (**Figure 1**). It is located in the south-east of the Gulf of Guinea at 4°67 south and 11°97 east, sheltered by a natural break, which is quite common in the area of the coast facing an average of 320° - 140°, in front of a fairly well-developed continental shelf about 40 km wide up to the 100-meter isobath [2] [3] [9]-[11]. This coastal zone is characterized by a sandy beach bordered by the Atlantic Ocean, with a gently sloping bathymetry [12].

## 2.2. Data

### 2.2.1. Bathymetry

The numerical simulation of a hydro-sedimentary process in a coastal zone relies on the accuracy of bathymetric data [12]. In this article, bathymetric data are provided by a terrain model for the ocean and land at 30-second arc intervals. This is the general bathymetric map of the oceans, GEBCO\_08 grid. These data are retrieved from an xyz file with x and y representing the geographical coordinates of the point and z its altitude. Negative elevations show water depths and positive elevations show topographic heights above water. The bathymetric map of the study area is shown in **Figure 2** [4].

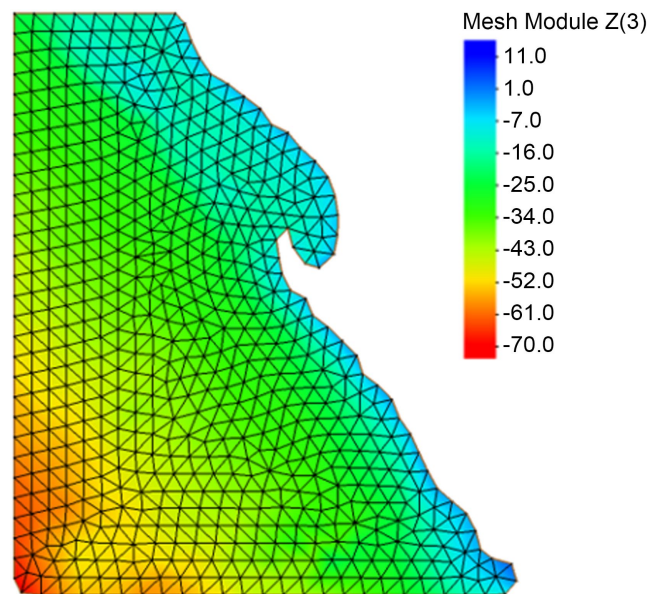


**Figure 2.** Bathymetry of the Pointe-Noire coastal area [2].

### 2.2.2. Sedimentology

Along the coast of Pointe-Noire and in the immediate offshore area, the surface layer sediments consist mainly of mangrove peat and alluvial sand [13].

The median diameter of foreshore sediments is 0.3 to 0.5 mm along the outer breakwater of the wild coast and decreases towards the open sea. At a depth of -10 m, off the wild coast, the median diameter is 0.10 mm and off the outer breakwater at the same depth, their diameter is 0.08 mm. Silt content increases from 5

to 30% between –10 and –15 m and from 30% to 80% beyond that. Towards the bend in the harbor, the grain size distribution is much more pronounced and is as follows: the largest diameter particles (between 0.15 and 0.30 mm) accumulate in the sand trap from the foreshore to a depth of –5 m; at depths of –5 to –10 m, the median diameter  $d_{50}$  remains between 0.10 and 0.15 mm; for depths beyond –10 m, it is less than 0.10 mm [13]. Within the bay, the median diameter  $d_{50}$  of sediments is between 0.10 and 0.15 mm [9].

The median diameter  $d_{50}$  in millimeters of beach sediments and seabed sediments can be presented by sector in **Table 1** [2] [9].

**Table 1.** Sectoral distribution of the median diameter  $d_{50}$  of sediments in the coastal zone of Pointe-Noire.

Longitude (decimal degree)	Latitude (decimal degree)	$d_{50}$ (mm)
11.825031	–4.795526	0.2
11.815021	–4.786978	0.15
11.799550	–4.773655	0.5
11.779986	–4.740618	0.15
11.787337	–4.755413	0.1
11.703306	–4.762461	0.3
11.724122	–4.898079	0.08

### 2.2.3. Wind

Variations in wind speed and direction influence the entire wave propagation process. The wind data used in this study was provided by the Pointe-Noire Ca-baigne and De Glisse marine weather stations. These weather stations are satellite models that predict wave speeds, directions, and heights at one-hour intervals. For simulations, we used a series of 22-hour data sets, a series of 72-hour data sets, and a series of 7-day data sets.

## 2.3. Method

Modeling of wave propagation and sediment transport in the coastal zone of Pointe-Noire is undertaken using the integrated Coastal Modeling System (CMS), which contains two modules: CMS-Wave, which deals with wave propagation, and CMS-Flow, which deals with hydrodynamics and sediment transport. These two models have proven highly effective in addressing wave propagation and sediment transport issues in coastal areas, functioning both separately and in combination [6] [7].

### 2.3.1. Wave Model

The model used for wave propagation is CMS-Wave. This is a phase-averaged spectral model for the propagation of irregular waves in coastal areas with com-

plex bathymetry. It is capable of simulating refraction, diffraction, reflection, shoaling, and wave breaking [7]. It determines the shear stress exerted by waves on the seabed. The theory behind this model is based on the wave action equilibrium equation [3] [14] [15].

The boundary conditions of the wave model consist of a spectral coverage in the southwest offshore, the southeast and northwest lateral boundaries that constitute the open boundaries, and the eastern boundary that corresponds to the rigid boundaries.

### 2.3.2. Hydro-Sedimentary Model

The hydro-sediment coupling, which takes into account tides, currents, and sediment transport, is handled by the CMS-Flow model. This model is governed by the equations of continuity and momentum.

When currents are assumed to be uniform with depth and in the presence of waves, the continuity (1) and momentum (2) equations are given by [16] [17]:

$$\frac{\partial h}{\partial t} + \frac{\partial(hV_j)}{\partial x_j} = S_M \quad (1)$$

And

$$\begin{aligned} & \frac{\partial(hV_j)}{\partial t} + \frac{\partial(hV_jV_i)}{\partial x_j} - \varepsilon_{ij}f_c hV_j \\ & = -gh \frac{\partial \bar{\eta}}{\partial x_i} - \frac{h}{\rho} \frac{\partial p_{atm}}{\partial x_i} + \frac{\partial}{\partial x_j} \left( v_i h \frac{\partial V_i}{\partial x_j} \right) \\ & - \frac{1}{\rho} \frac{\partial}{\partial x_j} (S_{ij} + R_{ij} - \rho h U_{wi} U_{wj}) + \frac{\tau_{si}}{\rho} - \frac{\tau_{bi}}{\rho} \end{aligned} \quad (2)$$

With,

- $f_c = 2\Omega \sin \phi$  Coriolis parameter in [rad/s], where  $\Omega = 7.29 \times 10^{-5}$  rad/s is the speed of the Earth's rotation and  $\phi$  is the latitude in degrees;
- $h = \bar{\eta} + d$  : total water depth averaged by waves, where  $\eta$  is the deformation of the water surface averaged in depth by waves in calm conditions and  $d$  water depth (positive downwards);
- $S_M$  : the term source and sink of water due to precipitation, evaporation, and structures;
- $V_i = U_i + U_{wi}$  : total flow velocity;
- $U_i$  : current velocity vector averaged by waves and depth (uniform depth);
- $U_{wi}$  : wave flow velocity vector;
- $v_i$  : total turbulent viscosity combined wave-current [ $m^2/s$ ];
- $\tau_{si}$  : the component of the vector constraint on the surface exerted by the wind [Pa];
- $\tau_{bi}$  : the shear stress component at the combined wave-current bottom [Pa];
- $R_{ij}$  : the stress tensor of the surface roller [Pa];
- $S_{ij}$  : wave radiation stress tensor [Pa];
- $\rho \approx 1025 \text{ kg} \cdot \text{m}^{-3}$  : density of seawater;

- $g$  : gravity in  $[m/s^2]$ ;
- $p_{atm}$  : atmospheric pressure  $[Pa]$ .

Sediment transport is governed by Equation (3), which represents the total transport of sediments of multiple sizes [7].

$$\frac{\partial}{\partial t} \left( h \frac{C_{tk}}{\beta_{tk}} \right) + \frac{\partial (h V_j C_{tk})}{\partial x_j} = \frac{\partial}{\partial x_j} \left[ v_s h \frac{\partial (r_{sk} C_{tk})}{\partial x_j} \right] + \alpha_i w_{sk} (C_{t^*k} - C_{tk}) \quad (3)$$

With  $j = 1, 2, \dots$  and  $k$  the size of the sediment class.

### 2.3.3. Boundary Conditions

#### 1) Boundary conditions for rigid walls (port and coastal structures and embankments)

The function used to simulate the additional flow drag due to the presence of coastal and port structures and banks, represented by its shear stress and modeled by Equation (4) [7]:

$$\tau_{wall} = - \frac{\rho u_*^w \kappa}{\ln(E y_p^+)} U_{\parallel} \quad (4)$$

With,

- $E$  : the wall roughness parameter;
- $y_p^+$  : the distance between the structure and point p;
- $u_*^w$  : the shear velocity at the wall;
- $\kappa = 0.4$ .

#### 2) Boundary condition at the water surface

Tide level forecasts are based on the official forecast formula of the United States National Oceanographic and Atmospheric Administration and the National Ocean Service in the USA, governed by Equation (5) [7]:

$$\eta(t) = \sum f_i A_i \cos(\omega_i t + V_i^0 + \bar{u}_i - \kappa_i) \quad (5)$$

With,

- $A_i$  : the average amplitude of tidal components;
- $f_i$  : node correction factor;
- $V_i^0 + \bar{u}_i$  : the equilibrium phase of the tidal constituents;
- $\kappa_i$  : phase shift.

#### 3) Boundary condition in coastal zone

Taking into account wave and wind forcing, along a cross-shore boundary there is a current along the shore. After simplification the momentum equation (2) reduces to Equation (6):

$$\frac{\partial}{\partial x_j} \left( v_t h \frac{\partial V_i}{\partial x_j} \right) = \frac{\tau_{si}}{\rho} + \frac{\tau_{wi}}{\rho} - \frac{\tau_{bi}}{\rho} \quad (6)$$

With,

- $q_i$  : the total flow;
- $n_B$  : the Manning coefficient at boundary B;

- $r$  : empirical constant equal to 2/3;
- $\Delta l$  : the transverse width of the cell.

#### 2.3.4. CMS-Wave/CMS-Flow Coupled Model

This coupling allows the interaction of all oceanic forcings (waves, tide and the currents they generate) acting in a coastal zone. It allows for a realistic assessment of the functioning of the hydrodynamic and sedimentary system. This coupling works in such a way that the variables transmitted from CMS-Wave to CMS-Flow are the significant wave height, the wave peak period, the wave direction, the breaking and the wave radiation stress, CMS-Wave uses the updated bathymetry (if sediment transport is enabled), the water levels and the current velocities provided by CMS-Flow [7] [18].

The boundary conditions of the coupled model are set by the conditions of the CMS-Wave wave model. These take into account the water level and currents generated by the waves on the one hand and by the tide on the other. They set the tidal conditions around the grid.

This approach involves solving the 1D continuity and momentum equations containing the radiation stress gradients along the axis normal to the boundary. The wave action along this axis is adjusted to the prescribed forcing values for water elevation at the boundary to provide consistent water level values at the boundary and within the grid [6] [7] [19].

The bed (bathymetry) of the Pointe-Noire coastal zone is sandy and gently sloping [12]. The most appropriate transport formula is that of Soulsby Van-Rijn [20]. This formula applies to total sediment transport (bed load and suspended load) under the combined action of waves and currents on horizontal and sloping beds. It is presented by Equation (8):

$$q_t = \rho_s A_s U \left[ \left( U^2 + 0.018 \frac{u_{rms}^2}{C_d} \right)^{0.5} - U_{cr} \right]^{2.4} \quad (8)$$

with,

- $q_t$  : total load transport [kg/m/s];
- $A_s = A_{sb} + A_{ss}$  : empirical coefficient;
- $A_{sb} = f_b \frac{0.005h \left( \frac{d_{50}}{h} \right)^{1.2}}{\left[ (s-1)gd_{50} \right]^{1.2}}$  : coefficient linked to transport by bedload;
- $A_{ss} = f_b \frac{0.012d_{50} (d_*)^{-0.6}}{\left[ (s-1)gd_{50} \right]^{1.2}}$  : coefficient related to suspended transport;
- $u_{rms}$  : mean orbital velocity of the wave at the bottom [m/s];
- $C_d = \left[ \frac{\kappa}{\ln \left( \frac{h}{z_0} \right) - 1} \right]^2$  : the drag coefficient due to current alone;

- $z_0 = 0.006$  m;
- $U_{cr}$ : the average critical velocity at depth for triggering sediment movement [m/s];
- $x_j$ : Cartesian coordinate of direction number  $j$  [m];
- $t$ : time [s];
- $C_{tk} = q_{tk}/Uh$ : the average depth concentration of the total sediment load for size class  $k$ ;
- $q_{tk}$ : the transport of the total load;
- $U$ : average current speed at depth [m];
- $\beta_{tk}$ : the total load correction factor;
- $r_{sk}$ : fraction of suspended sediment in the total load;
- $\nu_s$ : the horizontal mixing coefficient of sediments;
- $\alpha_t$ : total load adaptation coefficient;
- $w_{sk}$ : sediment fall velocity.

### 2.3.5. Setting up the Template and Getting Started with the SMS Software

The hydrodynamic and hydro-sedimentary modeling in the coastal zone of Pointe-Noire is undertaken by the CMS under the SMS software interface. The local model covers an area of 345.6 km<sup>2</sup>, from the Sauvage coast to Songolo beach including the port of Pointe-Noire, and is nested in a larger regional model [3]. The wave model used is that presented by Ndzessou *et al.*, (2025) [3]. These waves interact with the local hydro-sedimentary model reproducing the dynamics in the coastal zone linked to the tide, wind circulation and sediment dynamics, making it possible to simulate the morphological evolutions of the seabed by detecting erosion and sediment deposition zones using the CMS-Flow model.

The CMS-Wave model receives as input wave data at the boundary: significant height (m), direction (deg), peak wave period. It offers as output: height (m), dissipation, radiation stress gradient and wave breaking.

The CMS-Flow model receives as input data at the boundary for the hydro-sedimentary model: the tidal constituents specific to the coastal zone of Pointe-Noire, the new, the wind (direction and speed); the median diameter d50 of the sediments. It offers as output: the elevations of the water surface [m], current vector [m/s], evolution of the morphology of the bed, water depth, total load capacity of the sediments [kg/m<sup>3</sup>], the total concentration of sediment load [kg/(m·s)], fraction of sediment in suspension, eddy turbulent viscosity [m<sup>2</sup>/s].

The parameters of the sediment transport model are defined as follows:

- Solution scheme: Implicit;
- Matrix solver: GMRES;
- Combined wave-current bottom friction coefficient: quadratic wall friction;
- Bottom roughness type: Manning number (0.01);
- Turbulence model: Subgrid;
- Bottom current coefficient: 0.067;
- Formulation: Total non-equilibrium load;
- Transport formula: Soulsby-Van-Rijn;

- Sediment porosity: 0.4;
- Maximum number of bed layers: 10;
- Maximum bottom layer thickness: 0.05.

The wave and sediment transport models use the same grid, so interpolation is not required.

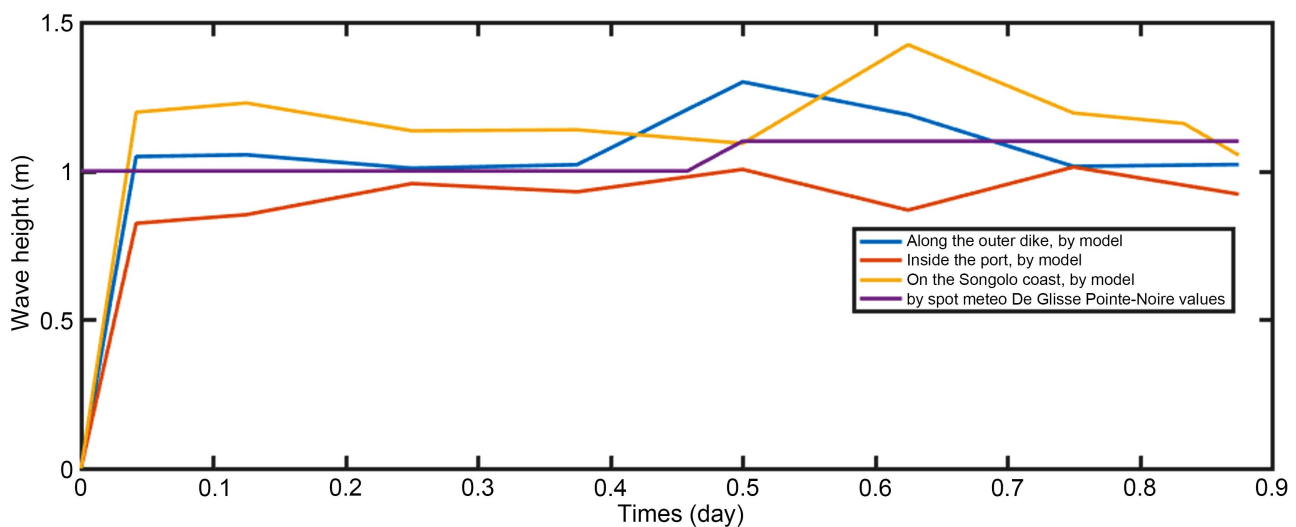
The models are coupled so that the wave outputs calculated by CMS-Wave are transmitted to CMS-Flow. Once sediment transport is enabled, CMS-Wave uses the updated bathymetry, water level, and current speeds provided by CMS-Flow for the next time step.

### 3. Results and Discussion

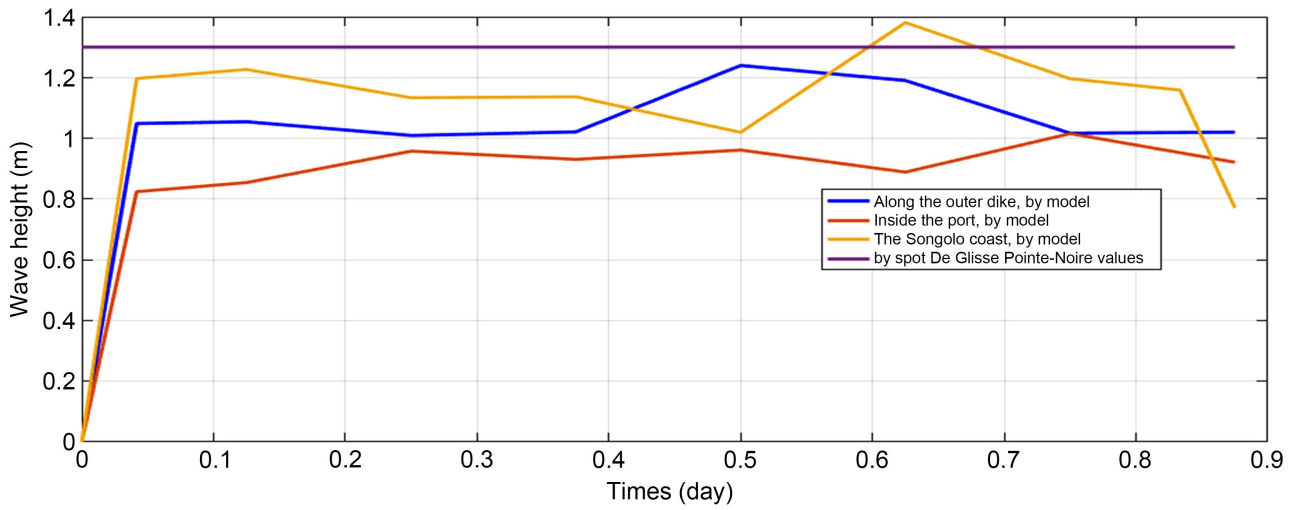
The presentation of the results is made in two parts, firstly the results of the separate models then those of the coupled model in order to allow the contribution of each element (wave, current, tide) to be detected in the dynamics of the coastal process of this site.

#### 3.1. Validation of the Wave Model

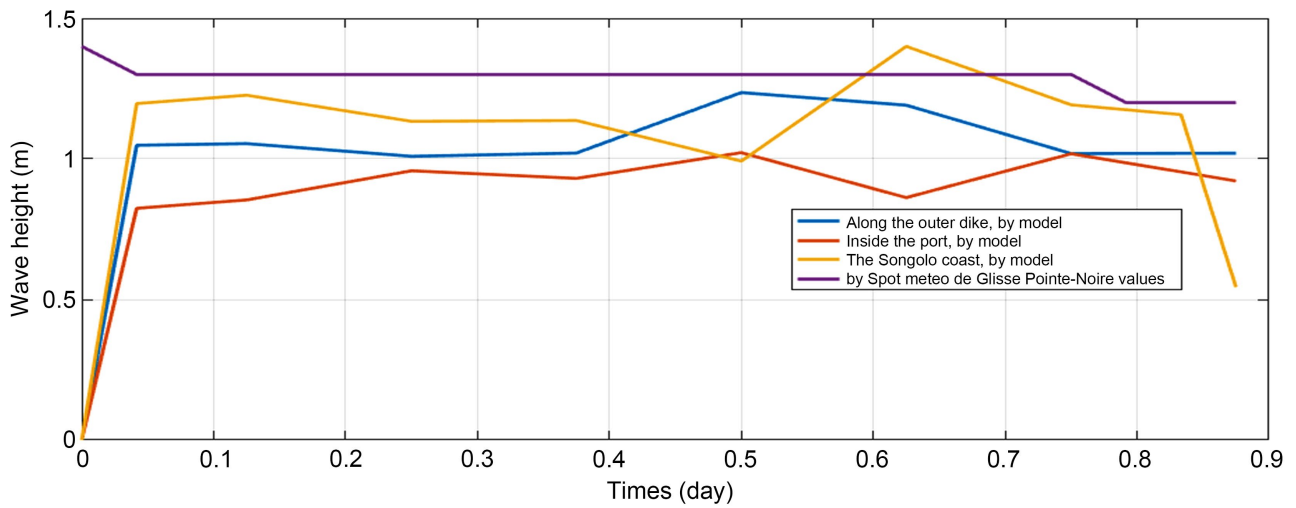
The De-glisse and Ça-Baigne marine weather forecasts use satellite images to predict wind speeds and directions, as well as wave heights and directions at the site. Digital models use the winds predicted by the weather forecasts as input data to simulate wave heights as output. Comparisons between the wave characteristics obtained from the digital model and those predicted by the marine weather spots validated the wave model used in the work of Ndzeou *et al.* (2025). The marine weather spots show the average wave height for the entire area over a one-hour interval. The model, on the other hand, allows the evolution of this wave height to be observed at all points in the study area. This comparison revealed a difference of between 0.1 m and 0.2 m (Figures 3(a)-(c) and Figure 3(d)). As these differences are very small, the model provides realistic and usable results.



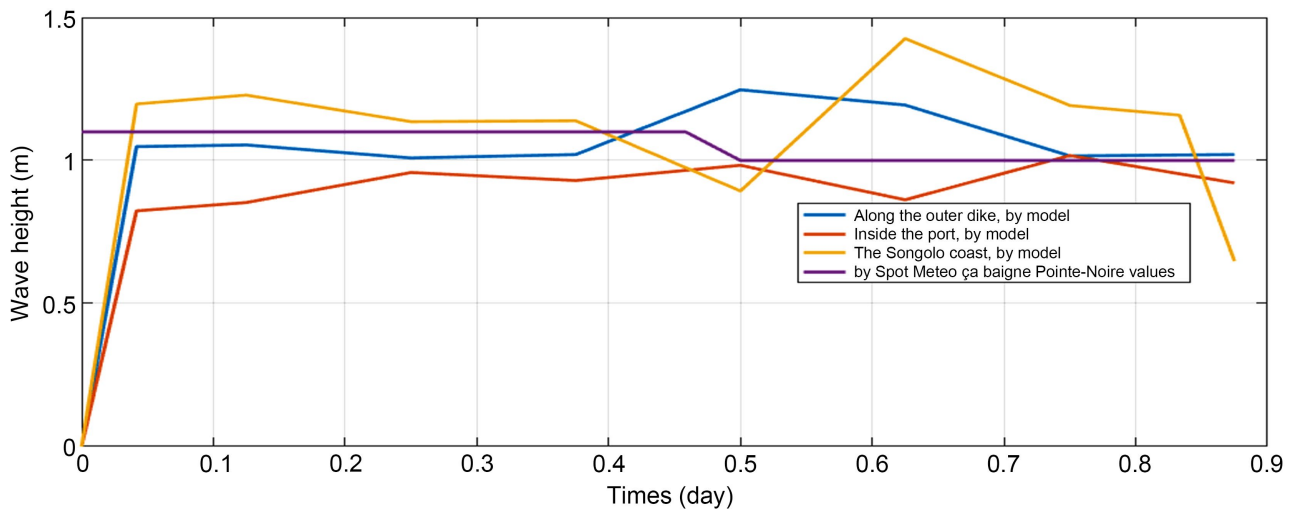
(a)



(b)



(c)



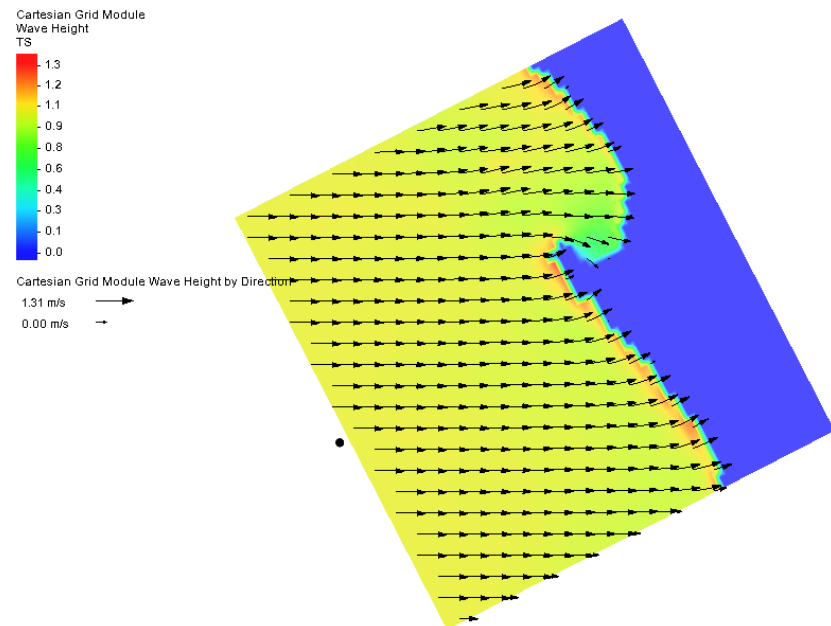
(d)

**Figure 3.** Comparison between the wave heights observed by the model and those predicted by the Deglisse and ça Baigne marine weather forecasts on June 23 and 24, 2024 [3].

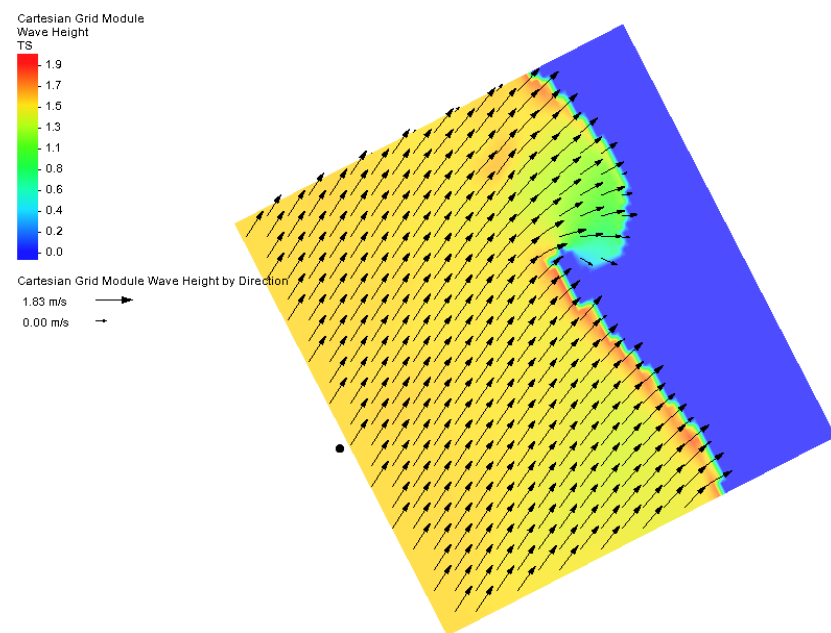
### 3.2. Swell and Waves

This method involved propagating project swells from the open sea towards the coast in oblique directions (northwest and southwest) and frontal to the coastline. This will enable analysis of wave behavior and understanding of their involvement in marine dynamics in this coastal area.

**Figure 4** shows the evolution of wave height in the coastal zone simulated by the CMS-Wave model in the three directions. Wave amplification is observed as the waves approach the shore for all three swell cases [3].



(a)



(b)

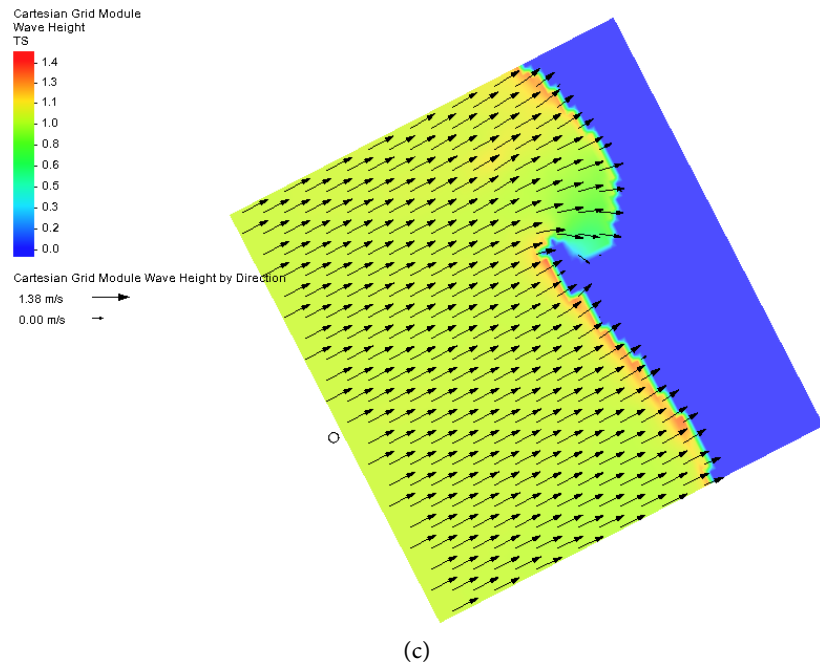


**Figure 4.** Changes in wave height in the coastal area of Pointe-Noire.

Swells with a southwesterly incidence are those with the greatest heights along the outer breakwater compared to those with a non-frontal incidence in the northwesterly and frontal directions; while in the Songolo area, the greatest heights are observed for northwesterly and frontal waves. The swell incidence angle has a very significant influence on the transformation of the swell and its effects near the coast.

**Figure 5** shows the direction taken by waves as they cross the coastal zone. For each swell case at the boundaries, a slight change in direction is observed, moving northward at the outer breakwater and at Songolo beach.

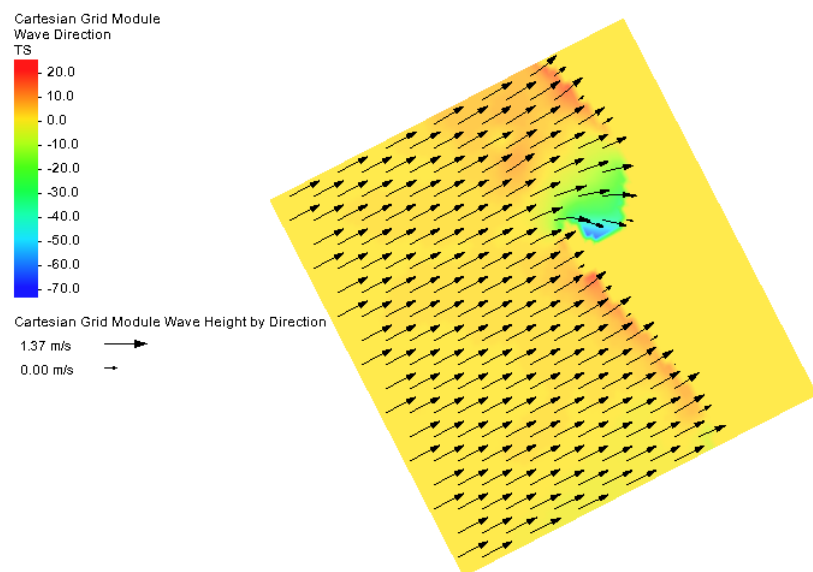


**Figure 5.** Evolution of wave direction approaching the coastal area of Pointe-Noire.

**Figure 6** simulates wave breaking in this area. Wave breaking in this coastal area is only observed at the Songolo coast and along the outer breakwater. This allows us to simultaneously assess the radiation stress at the bottom caused by waves; these effects are therefore zero offshore and increase very close to the coast. This hypothesis is confirmed by the increase in wave height at the same locations. These results are decisive in the hydro-sedimentary analysis.

The current configuration of the coastal zone and the presence of coastal and port structures have a significant impact on the transformations that waves undergo as they approach the coast of Pointe-Noire.

These various conclusions are supported by the study conducted by Ndzessou *et al.* (2025) [3].

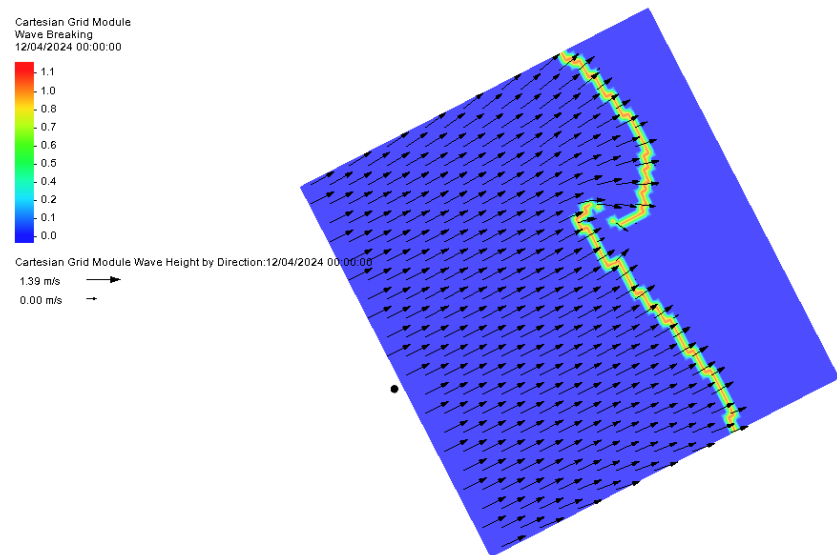


**Figure 6.** Wave braking.

### 3.3. Application of the CMS-Flow Model

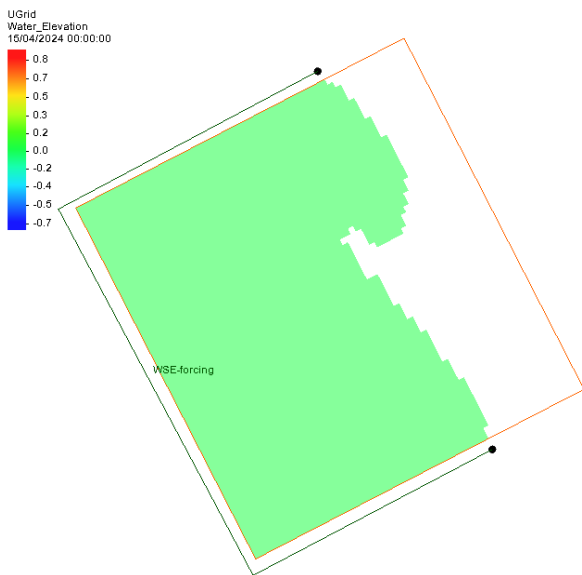
The application of the CMS-Flow model to the same grid as that of the wave model makes it possible to simulate the fluctuations of the tidal wave, the currents it generates as well as their impact on sediment dynamics. The parameterization of this model at the boundaries contains a WSE type forcing, the tidal constituents are of the semi-diurnal type M2, S2 and N2 (**Table 2**), the length of the BC type border is 49.207 km. This model makes it possible to read several hydrodynamic and hydro-sedimentary quantities, in particular the rise in sea level (the tidal amplitude), the amplitude of the currents, the evolution of the morphology of the bed, the concentration of the total sediment load near the bed and the fraction of suspended sediment.

**Figure 7** shows the sea level rises (the tide) over 24 hours. The different contour lines are observed at hourly intervals from 04/15/2024 at 00:00 to 04/16/2025. At 00:00 with the absence of the sun, corresponds to a stable level at 0.0 m. 6 hours later, the wave begins to gradually decrease to reach a first trough ( $-0.40$  m) at

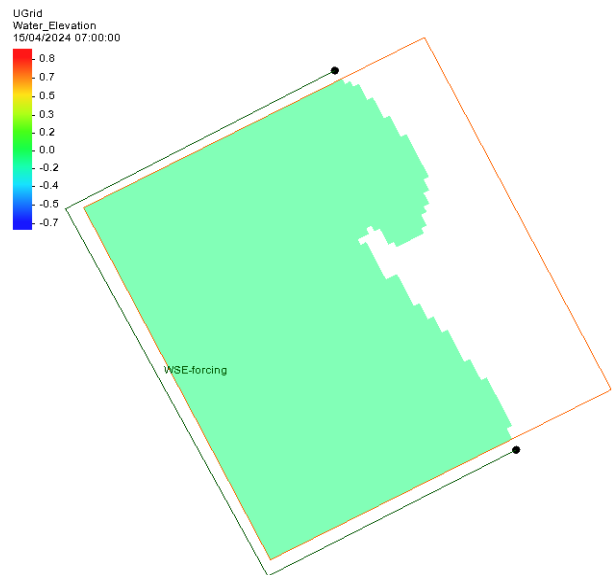
11:00. Then, the wave slowly increases to reach a first crest (+0.50 m) at 15:00. It passes through 0.0 m at 18:00 to reach a trough level (−0.50 m) at 21:00, it will then gradually increase to start again at 0.0 m at 0:00, thus the cycle will resume.

**Table 2.** Tidal boundary conditions.

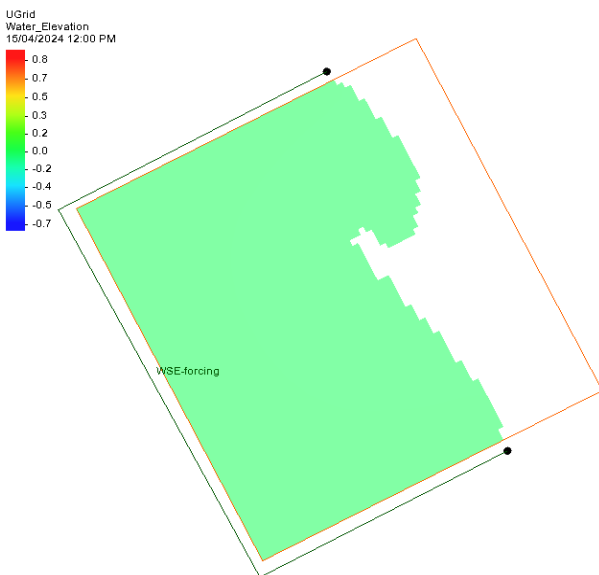
Tidal constituents	Amplitude (m)	Phase (°)
M2	1	15
S2	1	45
N2	1	60



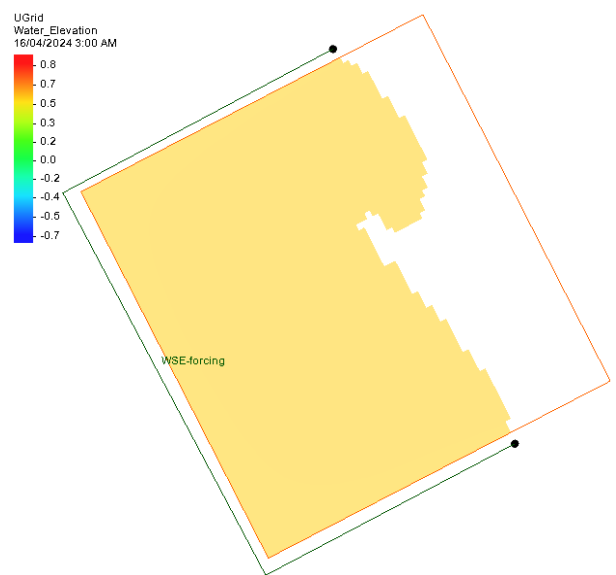
(a)



(b)



(c)



(d)

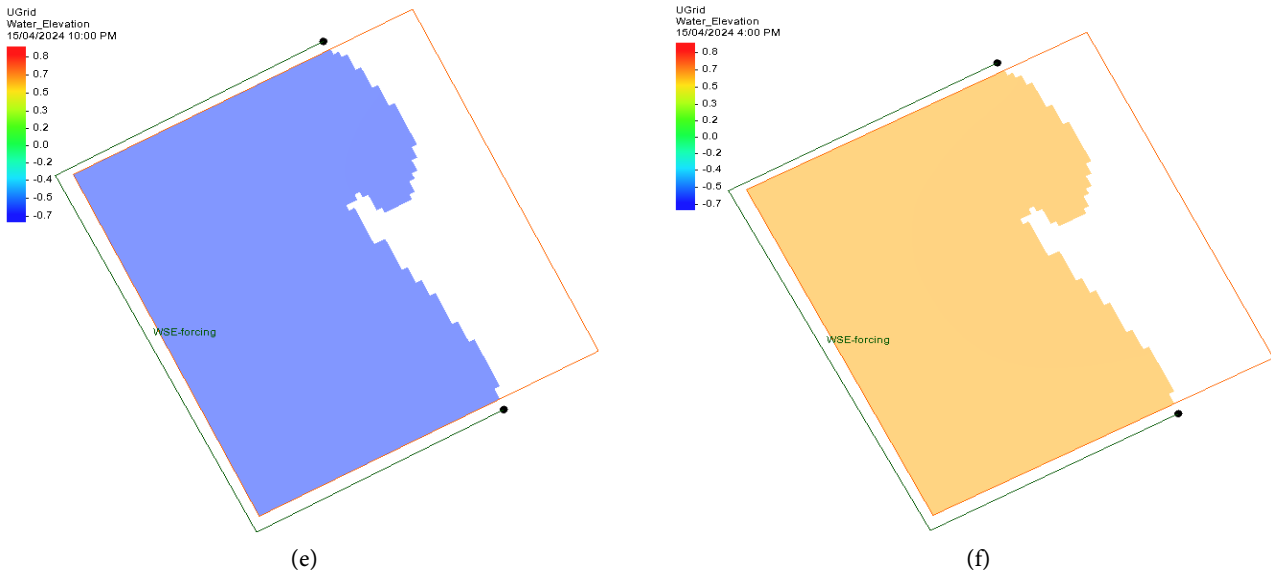
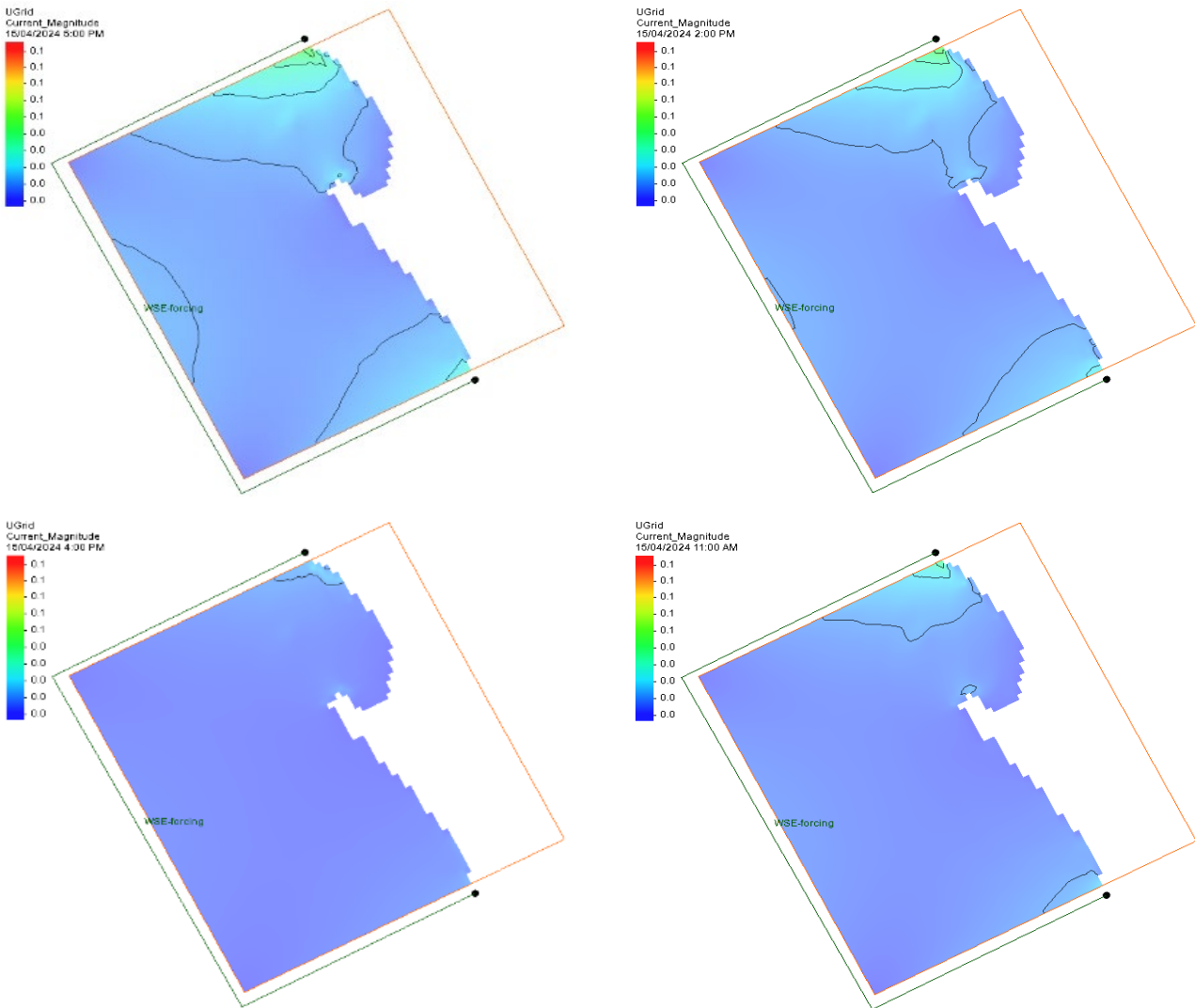
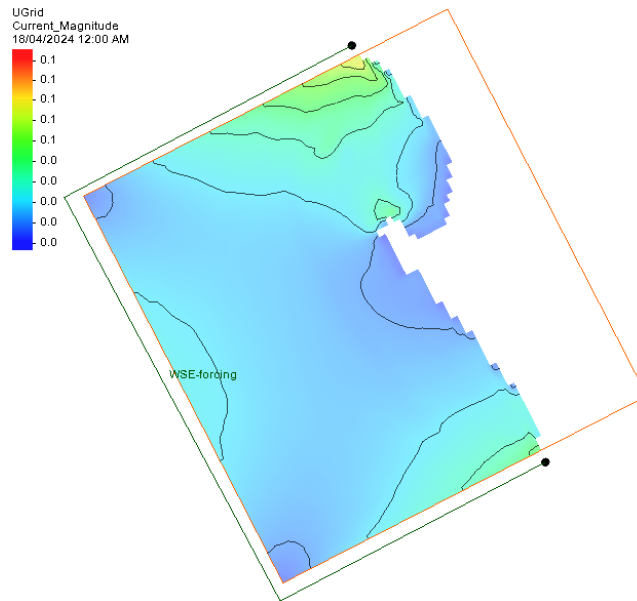


Figure 7. Water depth.





**Figure 8.** Amplitude of currents generated by tidal fluctuations in coastal areas.

**Figure 8** shows the evolution of currents generated by tidal fluctuations in the coastal area. During the day between noon and 1 p.m. and at sunset from 6 p.m. to 2 a.m., in the Songolo and Côte Sauvage area, a current with an amplitude of approximately 0.1 m/s appears. During the rest of the day, this current remains zero throughout the area.

**Figure 9** shows the evolution of the bed under the sole effect of the tides over three consecutive days. During these three days, no change in the bed is visible. Since the currents generated by the tide are weak, they do not cause the movement of sediments in this area.

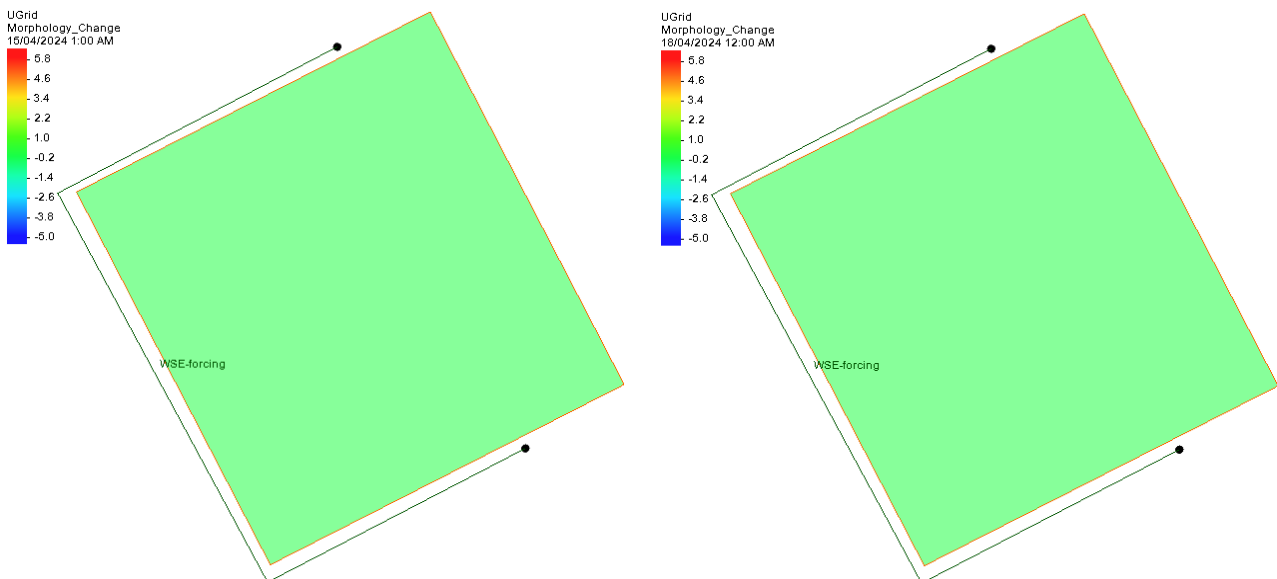


**Figure 9.** Evolution of the bed morphology.

### 3.4. Application of the Coupled Model to the Pointe-Noire Coastline

**Figure 10** and **Figure 11** show the sea level evolution simulated by the model over seven days and 30 days respectively. Analysis of these results allows us to propose the following tidal range:

- PMVE level: 1.60 m;
- PMME level: 1.30 m;
- BMME level: 0.40 m;
- BMVE level: 0.30 m;
- PBMA level: 0.00 m.

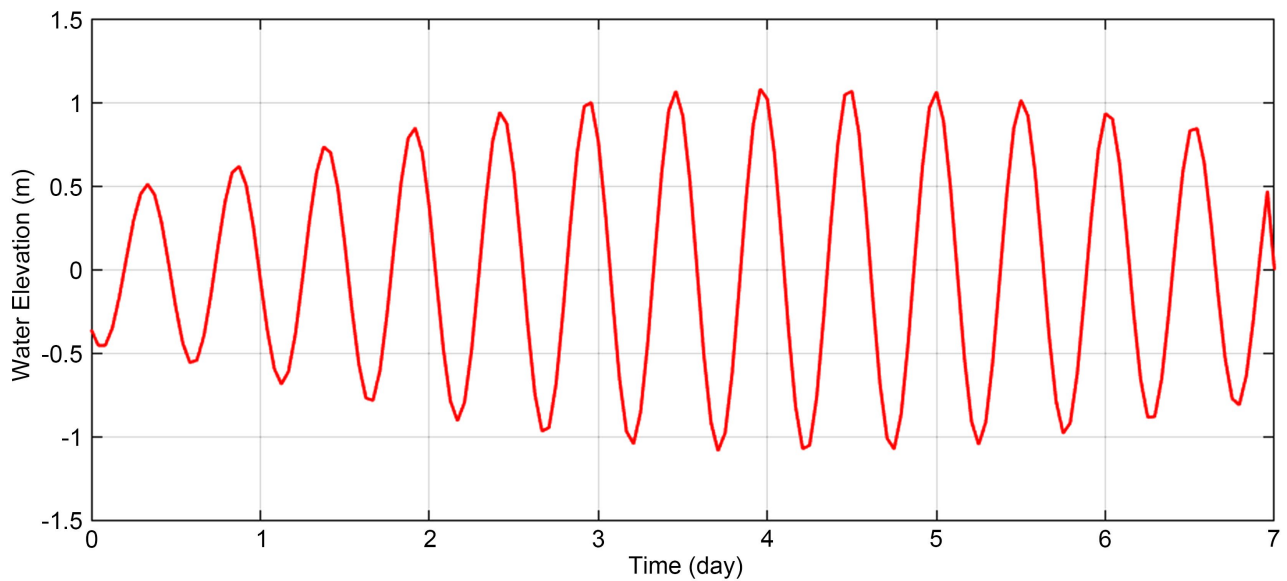


**Figure 10.** Water level changes over 7 consecutive days.

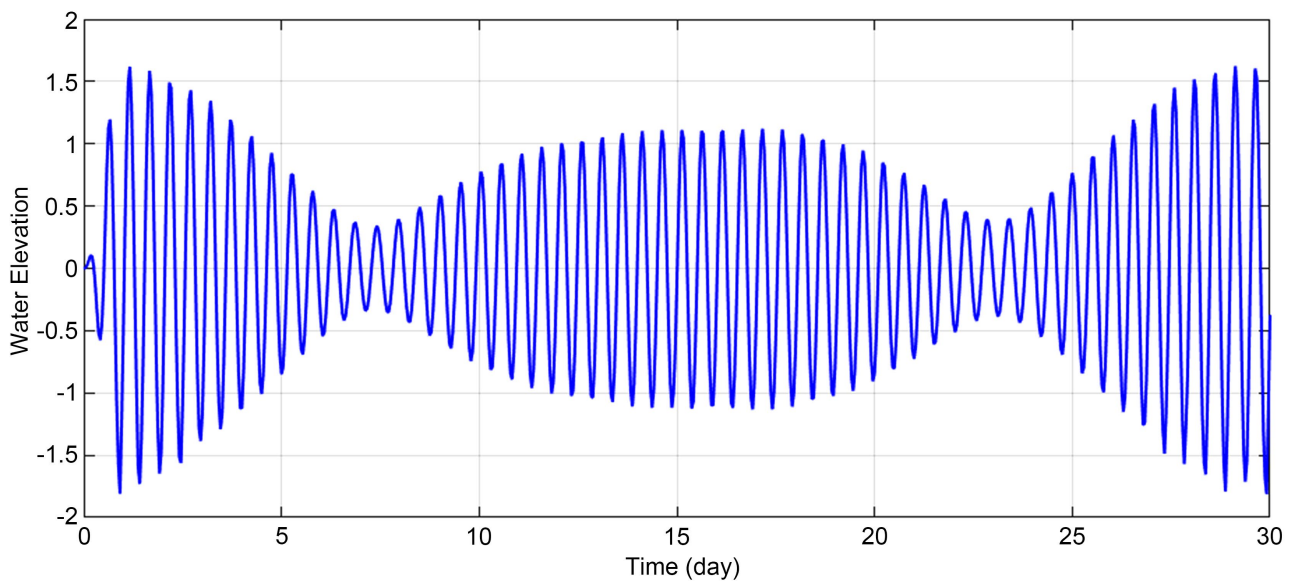


**Figure 11.** Water level changes over 30 consecutive days.

These results largely correspond to those presented in the report on the hydrology of the Autonomous Port of Pointe-Noire [9].

**Figure 12** presents the current amplitudes in three areas of the Pointe-Noire coast for a frontal swell with a significant height of 1.5 m. These observations show the highest peak in the Songolo area of approximately 1.7 m/s; along the breakwater, this peak is 0.9 m/s, while immediately offshore in front of the port, the peak is 0.3 m/s and very low, close to zero.

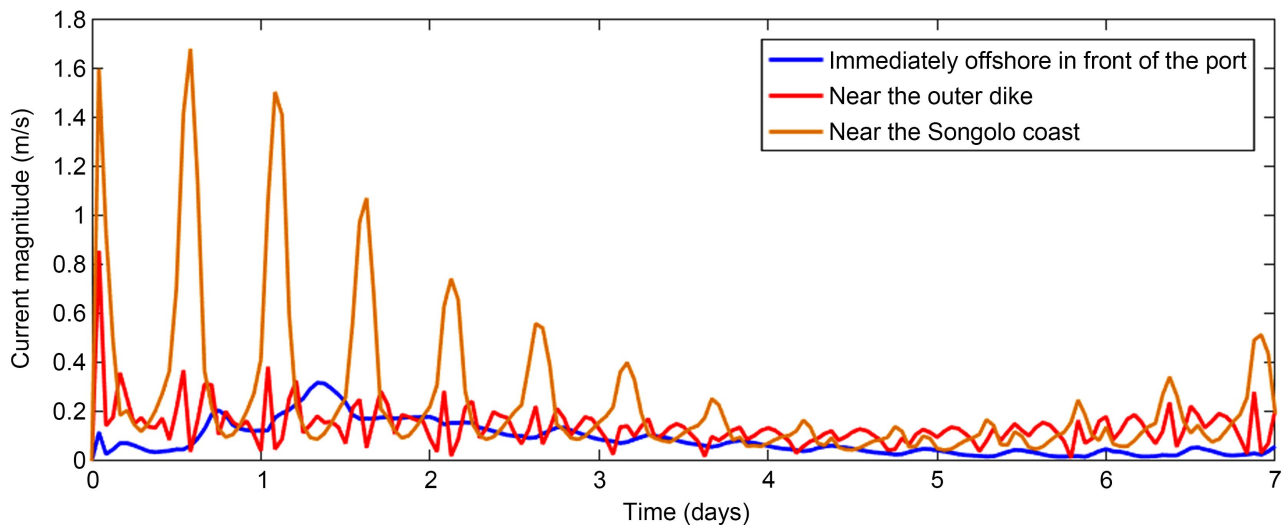


**Figure 12.** Amplitude of currents in m/s over three areas of the coast for 7 days for a frontal swell of  $H_s = 1.5$  m.

**Figure 13** simulated with an oblique (Southwest) swell with an incidence angle of  $30^\circ$  and a significant height of 1.5 m, records the highest current peak of 1.49 m/s in the Songolo area. Along the outer breakwater, the peak reached is 0.9 m/s. In the immediate offshore, these currents are very weak.

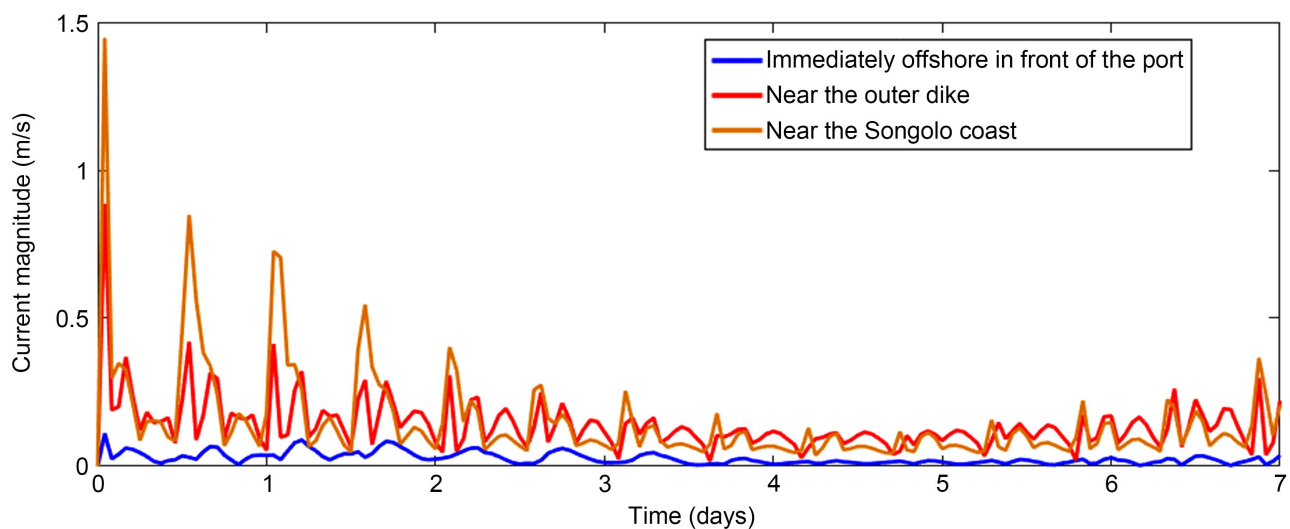


**Figure 13.** Amplitude of currents in m/s over three areas of the coast for 7 days for a swell with an angle of incidence of  $30^\circ$  and  $H_s = 1.5$  m.

When the incidence angle is  $-30^\circ$  (Northwest) for a significant height of 1.5 m, the highest current peak is 1.6 m/s, observed near the Songolo coast. Along the outer breakwater, the peak is 0.88 m/s (Figure 14).

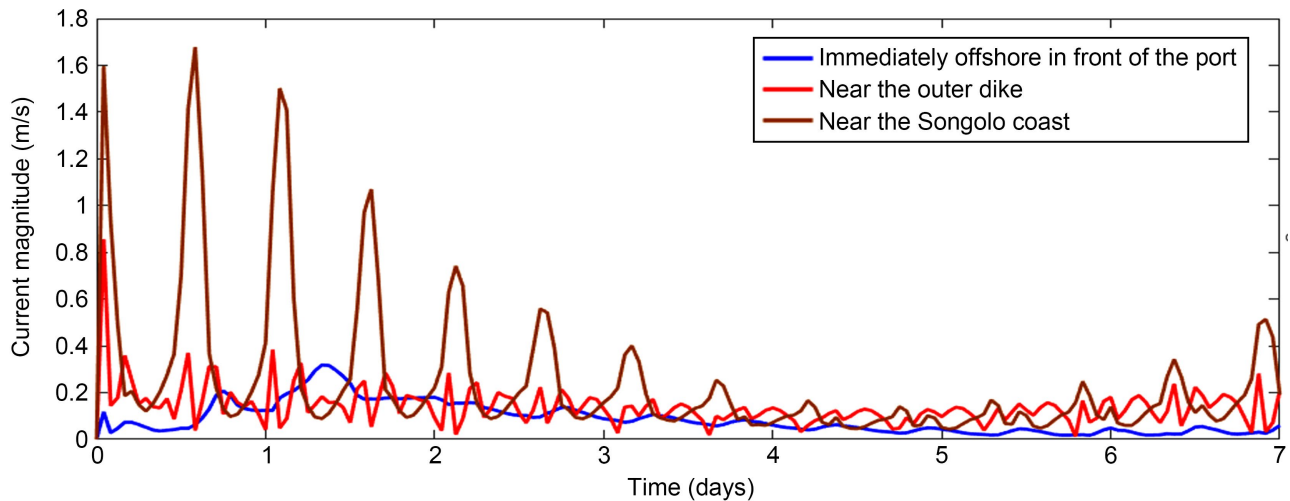


**Figure 14.** Amplitude of currents in m/s over three areas of the coast for 7 days for a swell with an angle of incidence of  $-30^\circ$  and  $H_s = 1.5$  m.

These different test cases show that, for the Pointe-Noire coastline, the frontal swell generates a current identical to that generated by the Northwest swell near the Songolo coast. It is slightly higher than that generated by the Southwest swell in the same area. When observed along the outer breakwater and towards the Côte Sauvage, this current is higher for a swell with a Southwest incidence angle.

The magnitude of the drift along the coast depends on the amplitude and angle of the incident wave, and the nature of the adjacent structure.

Figure 15 and Figure 16 present the evolution of the suspended sediment fraction for the two simulation cases. The simulation results show that sediments are suspended very close to the coast and along the outer breakwater. This is due to wave breaking occurring at the same locations. The suspended sediment fraction increases very rapidly from the beginning of the simulation and is maintained at above approximately 0.7 throughout the site.

The series of Figure 17, Figure 18, and Figure 19 simulate wave heights along the Pointe-Noire coast. The initial condition considered shows calm waters, followed by the appearance of very low waves that increase over time to reach their peak near the coast. Off the coast immediately in front of the port of Pointe-Noire, in the case of an oblique forcing in the southwesterly direction, the heights are slightly lower than those of a frontal and oblique swell in the northwesterly direction (Figure 20). The evolution of wave height in the case of a frontal swell is identical to that of a sloping swell in a northwesterly direction. At this level, there is a slight decrease in height compared to that measured at the border.

Along the outer breakwater, there is an amplification of the wave height with troughs that vary depending on the angle of incidence of the swell.

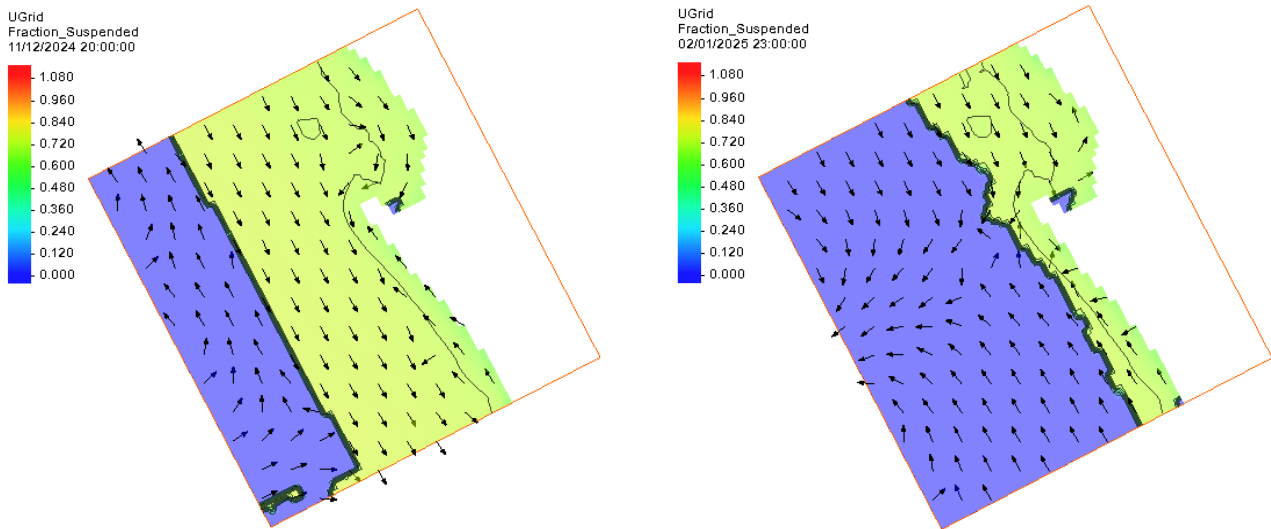


Figure 15. Fraction of suspended sediments; the arrows represent the direction of the flow field.

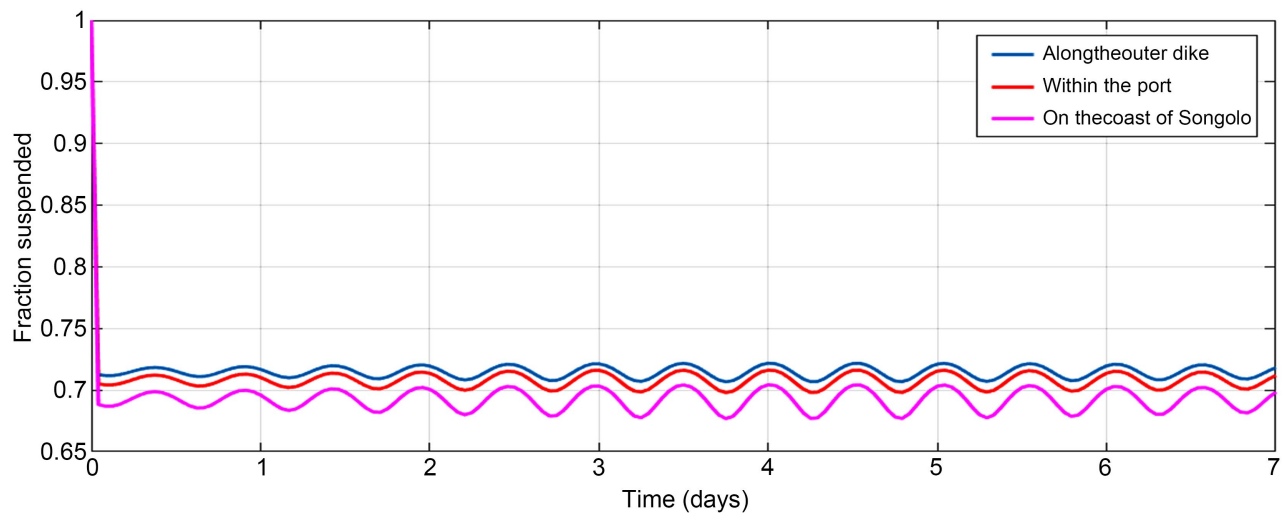
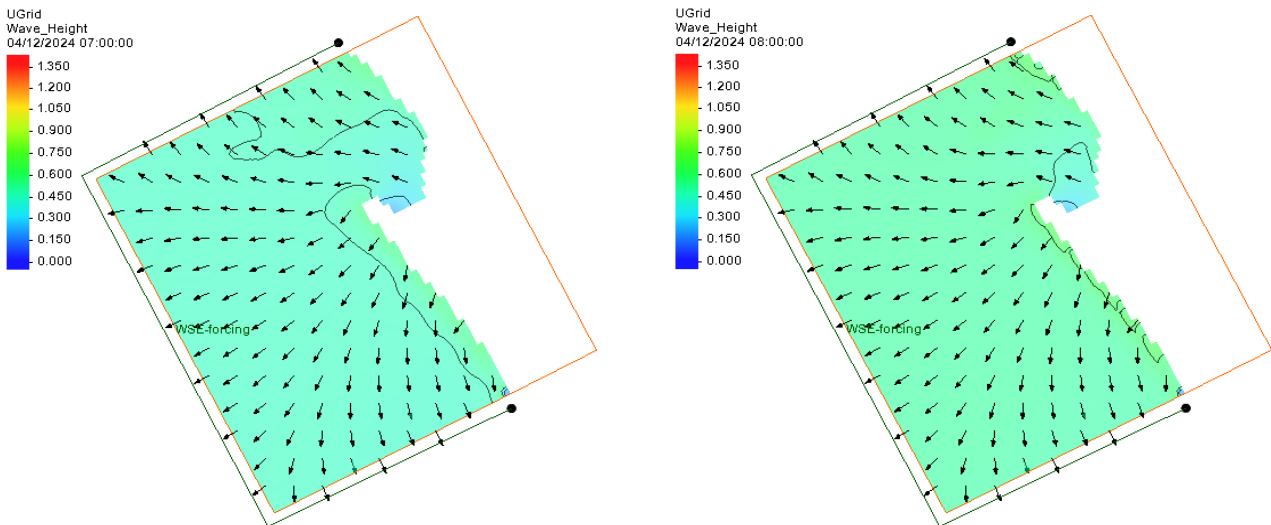
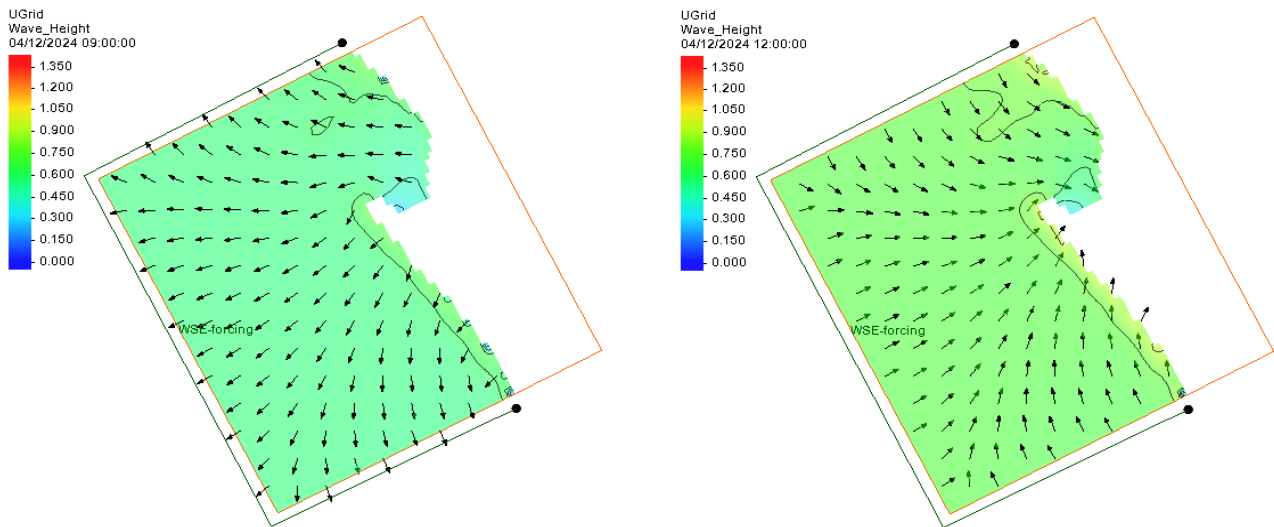
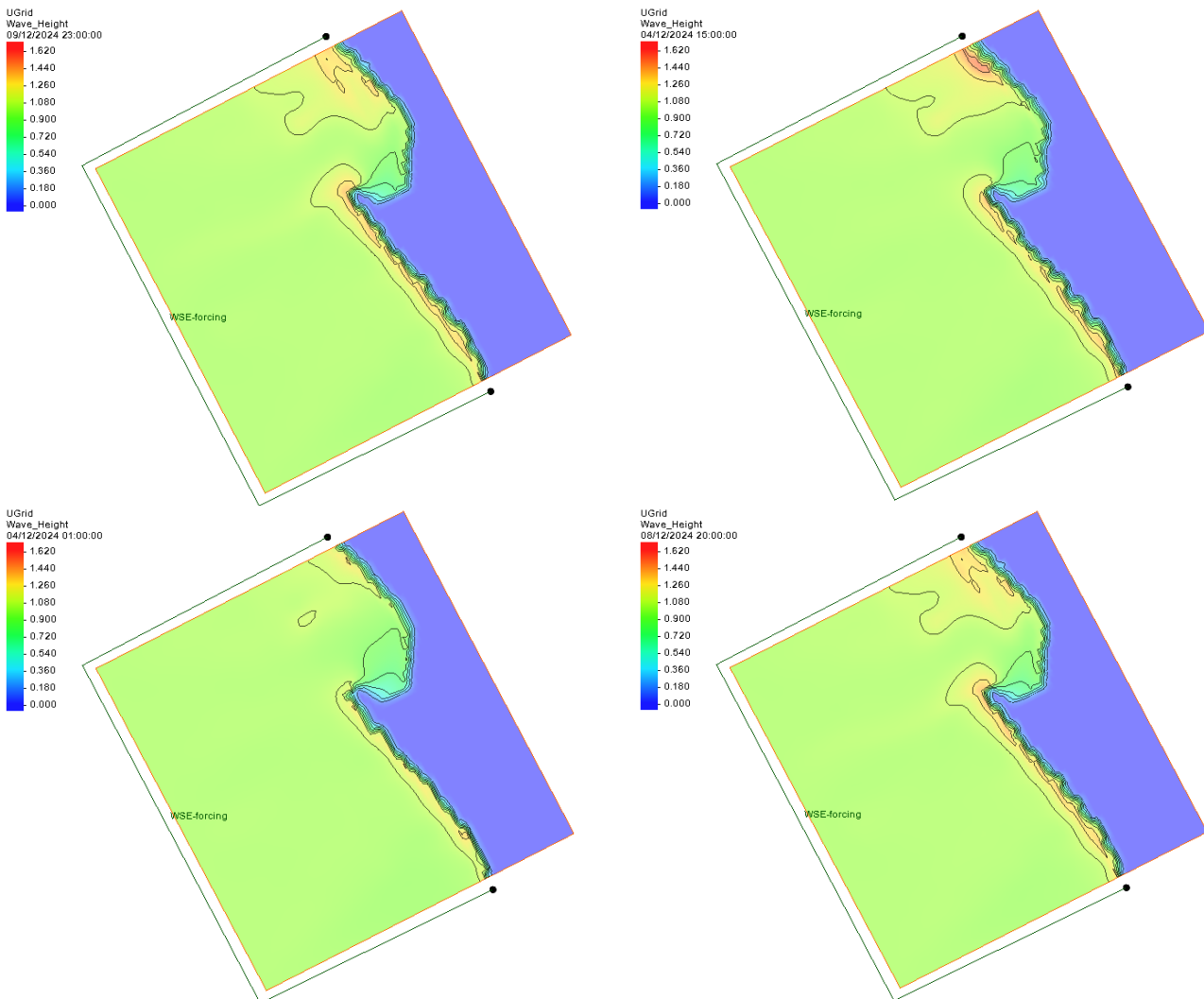


Figure 16. Fraction of suspended sediments in three areas of the coast over 7 days; the arrows represent the wind direction.





**Figure 17.** Wave height for a head-on swell of  $H_s = 1$  m; the arrows represent the direction of the flow field.



**Figure 18.** Wave height evolution along the entire coast for a swell with an angle of incidence of  $-30^\circ$  and  $H_s = 1.5$  m.

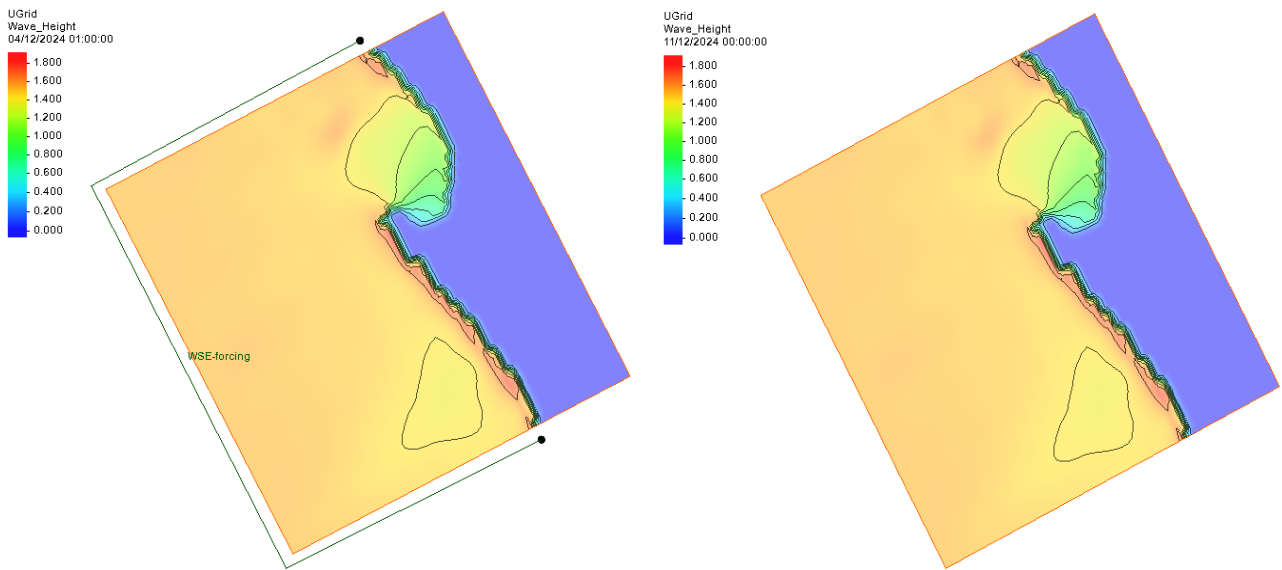


**Figure 19.** Wave height evolution along the entire coast for a swell with an angle of incidence of  $30^\circ$  and  $H_s = 1.5$  m.

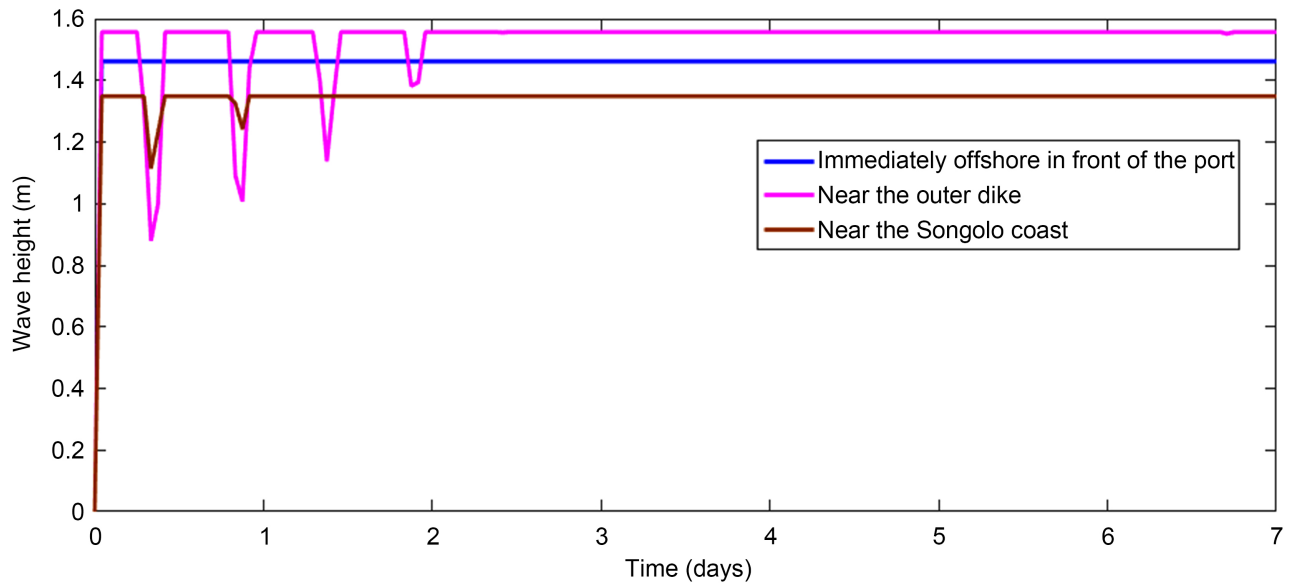


**Figure 20.** Wave height evolution over the three coastal areas for a head-on swell of  $H_s = 1.5$  m over 7 days.

**Figure 21** and **Figure 22** present the evolution of the bed morphology in the coastal zone simulated by the coupled model for seven (07) days (from 06/29/2024 to 07/06/2024). The results show that from the coupled model, the evolution of the bed is visible after 24 hours from the launch of the model. From **Figure 21**, it can be seen that the sediment transit is along the coast. The sediments transiting along the outer dike come from the Sauvage coast and those descending on the Northeast side of the port come from the Songolo beach. The curves in **Figure 22**, located below the x-axis ( $h = 0$  m), represent erosion points at the bed level, while those above the x-axis represent sediment deposition points. There is an almost exponential evolution of erosion and sediment deposition.

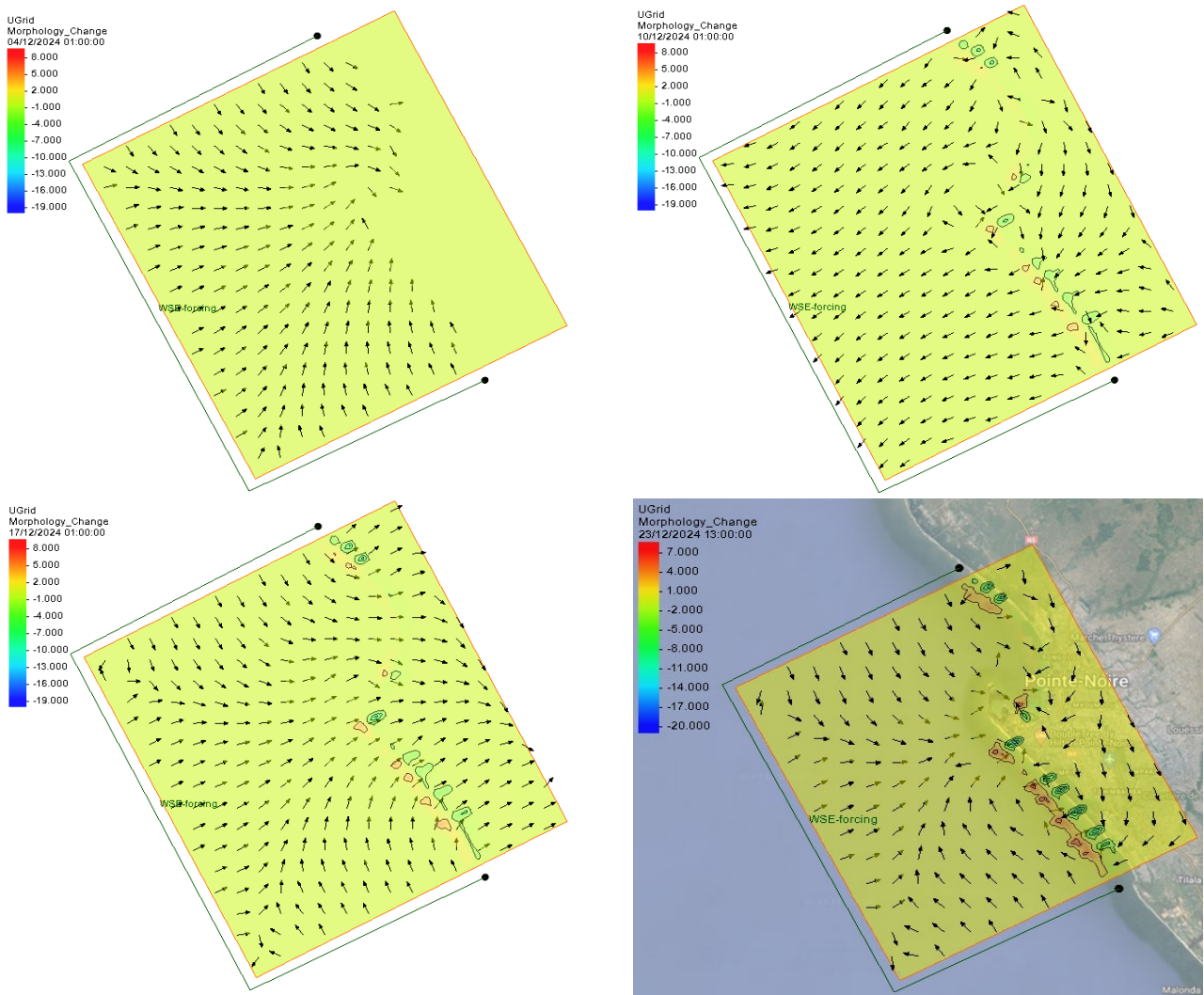


**Figure 21.** Evolution of the coastline morphology over 31 days; the arrows represent the direction of the flow field.

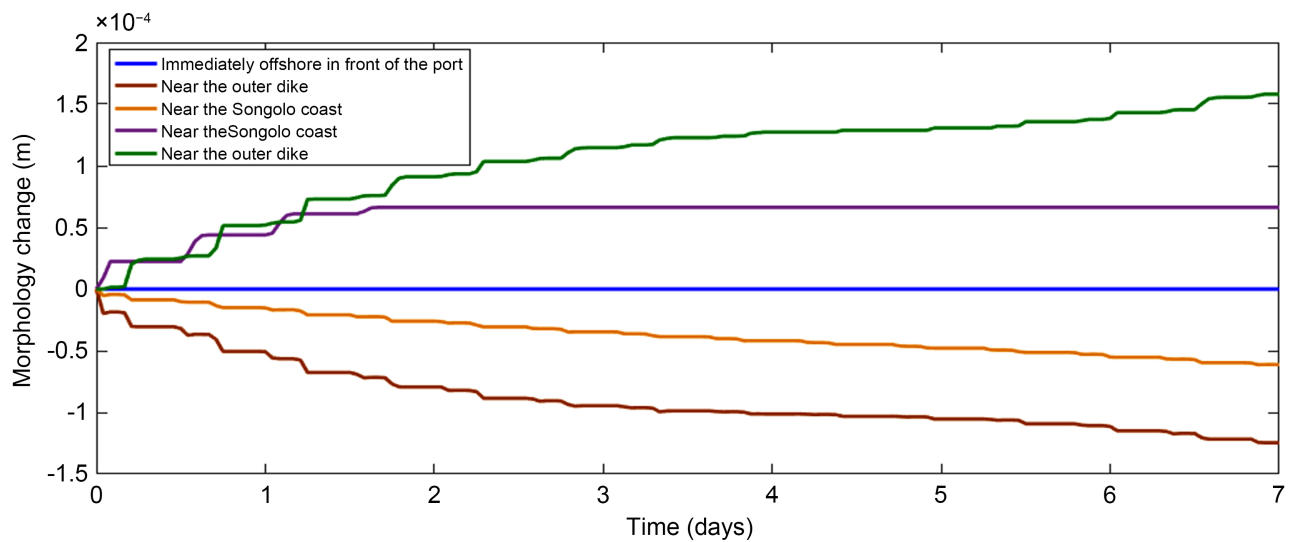


**Figure 22.** Identification of erosion and sediment deposition points on the coast over a period of 7 days.

The sand trap zone located at the end of the port's protective breakwater is largely supplied by sediment (sand) from the Côte Sauvage (southeast of the port) under the drainage of drift currents generated by the southwest swell, which remains almost permanent.

Hydrodynamic and sedimentary studies conducted by certain authors in the coastal zone of Pointe-Noire reveal the following:

1) Along the entire coast, the tidal ranges are relatively small: 1.4 m in spring tide and 0.8 m in neap tide for Pointe-Noire [21]; whereas according to the technical report of the call for tenders for the dredging of the port of Pointe-Noire in 2014, the values of the water heights are as follows: NPMVE: 1.5 m, NPMME: 1.3 m; NM: 0.9 m (in comparison, for this study, we find values similar to those obtained in the report [9]).

2) At the port of Pointe-Noire, the sand transit is of the order of 300,000 to 400,000 m<sup>3</sup>/year according to Giresse (1980) [21] and of 200,000 to 300,000 m<sup>3</sup>/year according to the 2014 annual report on hydrography in the Republic of Congo [1]. This significant drift is at the origin of the modeling of this almost always rectilinear sandy coastline: the results obtained in the context of the present study estimate the sediment transport of the order of 15,775.5 m<sup>3</sup>/month. These are close to the results of the 2014 report.

#### 4. Conclusions

This study highlights the importance of an integrated approach to hydrodynamic and sediment analysis in the coastal area of Pointe-Noire. It has made it possible to detect, to some extent, areas prone to erosion by highlighting high current peaks and also the origin of sand obstructing the port access channel.

The use of wave and hydro-sedimentary models, both separately and in combination, has made it possible to understand the contribution of each of these phenomena (tide, current, waves) to the dynamics of the coastal system in this area. Indeed, waves are the only drivers of sediment movement. Tidal currents are not the only ones capable of moving sediment in this area.

This study provides some insights into the origins of the erosion occurring in Loango Bay around the village of Matombi.

The coastal area of Pointe-Noire is exposed to swells coming from the southwest. In order to significantly reduce the flow of sediment traveling along the outer dike from the Côte Sauvage and depositing in the sand trap, a solution aimed at mitigating the energy of the southwest swell by installing an auxiliary structure (breakwater) could be considered.

Future research must incorporate the effects of climate change at the regional level, particularly sea level rise and changes in storm patterns, in order to improve forecasting capabilities.

#### Conflicts of Interest

The authors declare no conflicts of interest regarding the publication of this paper.

## References

- [1] Rapport annuel sur l'hydrographie en république du Congo (2014) Rapport technique du ministère délégué chargé à la Marine Marchande.
- [2] Ndzessou, W.B. (2024) Modélisation de la propagation de la houle et du transport de sédiments en zone côtière et portuaire de Pointe-Noire. Master's Thesis, Université Marine Ngouabi (Congo).
- [3] Ndzessou, W.B., Etou, D.G., Bockou-Ekockaut, J.A. and Tathy, C.A.A. (2025) Numerical Modeling of Swell Transformation as It Approaches the Coast of Pointe-noire. *Open Journal of Marine Science*, **15**, 100-113. <https://doi.org/10.4236/ojms.2025.152006>
- [4] Buttolph, A.M., Reed, C.W., Kraus, N.C., Ono, N., Larson, M., Camenen, B., Hanson, H., Wamsley, T. and Zundel, A.K. (2006) Two Dimensional Depth-Averaged Circulation Model CMS-m2D: Version 3.0, Report 2: Sediment Transport and Morphology Change. ERDC/CHL TR-06, 9.
- [5] Lin, L., Demirbilek, Z., Mase, H., Yamada, F., Zheng, J., *et al.* (2008) CMS-Wave: A Nearshore Spectral Wave Processes Model for Coastal Inlets and Navigation Projects. Coastal and Hydraulics Laboratory.
- [6] Reed, C.W., Brown, M.E., Sánchez, A., Wu, W. and Buttolph, A.M. (2011) The Coastal Modeling System Flow Model (CMS-Flow): Past and Present. *Journal of Coastal Research*, **59**, 1-6. <https://doi.org/10.2112/si59-001.1>
- [7] Sanchez, A., Beck, T., Lin, L., Demirbilek, Z., *et al.* (2012) Coastal Modeling System Draft User Manual. Coastal and Hydraulics Laboratory.
- [8] Militello, A., Reed, C.W., Zundel, A.K., Kraus, N.C., *et al.* (2004) Two-Dimensional Depth-Averaged Circulation Model m2D: Version 2.0, Report 1, Technical Documentation and User's Guide. Coastal and Hydraulics Laboratory.
- [9] PAPN (2014) Dossier d'appel d'offres pour les travaux de dragage pour l'accès nautique au port. Technical report, Port Autonome de Pointe-Noire.
- [10] Leroux, M. (1975) Climatologie dynamique de l'Afrique. *Travaux et Documents de Géographie Tropicale*, **19**, 87-112.
- [11] Samba, G. and Mpounza, M. (2005) Application du processus de Markov sur les occurrences des précipitations journalières au Congo-Brazzaville. *Comptes Rendus. Géoscience*, **337**, 1355-1364. <https://doi.org/10.1016/j.crte.2005.07.010>
- [12] Ndzessou, W., Tathy, C. and Etou, D. (2023) Contribution to the Modeling of Wave Propagation in the Coastal and Harbor Area of Pointe-Noire. *American Journal of Engineering Research*, **12**, 77-85.
- [13] Sofreco-CERAP (2004) Etude du secteur agricole—République du Congo, monographie du département de Pointe-Noire.
- [14] Mase, H. (2001) Multi-Directional Random Wave Transformation Model Based on Energy Balance Equation. *Coastal Engineering Journal*, **43**, 317-337. <https://doi.org/10.1142/s0578563401000396>
- [15] Sanchez, A., Wu, W., Li, H., Brown, M.E., Reed, C.W., Rosati, J.D., Demirbilek, Z., *et al.* (2014) Coastal Modeling System: Mathematical Formulations and Numerical Methods. Coastal and Hydraulics Laboratory.
- [16] Mei, C.C. (1989) The Applied Dynamics of Ocean Surface Waves, volume 1. World Scientific.
- [17] Svendsen, I.A. (2005) Introduction to Nearshore Hydrodynamics. World Scientific. <https://doi.org/10.1142/5740>

- [18] Tessier, C., Vested, H.J., Christensen, B.B., Goubert, E. and Salaün, F. (2012) Modélisation numérique de la dynamique sédimentaire de l'estuaire de la Vilaine. *XI<sup>èmes</sup> Journées*, Cherbourg, 12-14 July 2012, 471-480. <https://doi.org/10.5150/jngcgc.2012.051-t>
- [19] Bakshi, S. and Bhar, K.K. (2020) Simulation of Tidal Morpho-Dynamics in the Hooghly Estuary Using CMS Flow and Artificial Neural Network Models. *Procedia Computer Science*, **167**, 459-467. <https://doi.org/10.1016/j.procs.2020.03.255>
- [20] Soulsby, R.L. and Whitehouse, R. (1997) Threshold of Sediment Motion in Coastal Environments. *6th Australasian Port and Harbour Conference*, Christchurch, 1 January 1997, 145-150.
- [21] Giresse, P. (1980) Carte sédimentologique du plateau continental. Technical report, ORSTOM.